

Original Article

Endogenous HMGB1 regulates GSDME-mediated pyroptosis via ROS/ERK1/2/caspase-3/GSDME signaling in neuroblastoma

Chen-Ying Fan¹, Fang-Hua Ye¹, Min Peng¹, Jia-Jia Dong¹, Wen-Wen Chai², Wen-Jun Deng¹, Hui Zhang¹, Liang-Chun Yang¹

¹Department of Pediatrics, Xiangya Hospital, Central South University, Changsha 410008, Hunan, The People's Republic of China; ²Department of Nuclear Medicine, Hunan Cancer Hospital/The Affiliated Cancer Hospital of Xiangya School of Medicine, Central South University, Changsha 410008, Hunan, The People's Republic of China

Received October 1, 2022; Accepted January 26, 2023; Epub February 15, 2023; Published February 28, 2023

Abstract: Pyroptosis, a newly discovered mode of programmed cell death (PCD), is important in the regulation of cancer development. High mobility group box 1 (HMGB1) is a non-histone nuclear protein that is closely related to tumor development and chemotherapy resistance. However, whether endogenous HMGB1 regulates pyroptosis in neuroblastoma remains unknown. Here, we showed that HMGB1 showed ubiquitous higher expression in SH-SY5Y cells and clinical tumors, and was positively correlated with the risk factors of patients with neuroblastoma. Knockdown of GSDME or pharmacological inhibition of caspase-3 blocked pyroptosis and cytosolic translocation of HMGB1. Moreover, knockdown of HMGB1 inhibited cisplatin (DDP) or etoposide (VP16)-induced pyroptosis by decreasing GSDME-NT and cleaved caspase-3 expression, resulting in cell blebbing and LDH release. Knockdown of HMGB1 expression increased the sensitivity of SH-SY5Y cells to chemotherapy and switched pyroptosis to apoptosis. Furthermore, the ROS/ERK1/2/caspase-3/GSDME pathway was found to be functionally connected with DDP or VP16-induced pyroptosis. Hydrogen peroxide (H₂O₂, a ROS agonist) and EGF (an ERK agonist) promoted the cleavage of GSDME and caspase-3 in DDP or VP16 treatment cells, both of which were inhibited by HMGB1 knockdown. Importantly, these data were further supported by the in vivo experiment. Our study suggests that HMGB1 is a novel regulator of pyroptosis via the ROS/ERK1/2/caspase-3/GSDME pathway and a potential drug target for therapeutic interventions in neuroblastoma.

Keywords: HMGB1, pyroptosis, neuroblastoma, GSDME

Introduction

Neuroblastoma is a cancer that arises in cells derived from the neural crest, and tumors can develop at any site in the sympathetic nervous system. Neuroblastoma is a complex and heterogeneous disease, with diverse factors known to participate in its pathogenesis and development [1]. Most children are diagnosed under the age of 5 years, with a median age at diagnosis of 17 months. Clinical symptoms vary depending on the location of the primary tumor, and may include an abdominal mass, abdominal pain, respiratory distress, or neurological symptoms from spinal cord involvement [2]. With the continuous development and standardization of anti-tumor therapy, the survival

rate of low and medium-risk children has significantly improved through comprehensive treatment such as surgery, chemotherapy, and radiotherapy. However, the prognosis of high-risk children is still poor, with relapse, drug resistance, and distant metastasis all common in the later stage [2, 3]. Therefore, the mechanisms of resistance and relapse of pediatric neuroblastoma require more intensive investigation and the search for novel therapeutic strategies.

Pyroptosis is a newly identified programmed cell death (PCD), characterized by cell swelling, formation of large bubbles on the plasma membrane and disruption of plasma membrane [4]. Physiologically, pyroptosis serves as an initiator

Endogenous HMGB1 regulates pyroptosis in neuroblastoma cells

of innate immunity by inducing the release of cytokines, including IL-1 β and IL-18, and other molecules, such as HMGB1 and ATP, after cell membrane rupture [5, 6]. Gasdermin proteins are one of the main families of proteins involved in pyroptosis, and their cleavage fragments insert into the cell membrane [7]. GSDME-mediated pyroptosis plays important roles in the modulation of cancer progression and chemotherapy [8]. GSDME inactivation due to hypermethylation of the promoter has been detected in 50% of primary gastric cancers and supports the notion of GSDME as a putative tumor suppressor [9]. Transcription of GSDME increased in response to p53 activation, where it is believed to serve as a putative tumor suppressor and can inhibit the occurrence and development of cancers [10]. Recently, study has demonstrated chemotherapy drug (Topotecan, VP16, DDP or CPT-11)-induced GSDME-mediated pyroptosis in SH-SY5Y cells causes rapid cell death [11]. And GSDME expression was also decreased in VP16-resistant melanoma cells and was negatively associated with cell resistance to VP16-induced cell death [12]. Moreover, GSDME is involved in chemotherapy-induced pyroptosis in tumor cells, which requires the activation of caspase-3 [11, 13]. GSDME significantly promotes the caspase-3/9 pathway in melanoma and colon cancer cell lines [14, 15]. These studies indicate that exploring the role of pyroptosis in the pathogenesis of human cancers may provide new ideas and effective therapeutic targets for cancer prevention and treatment.

HMGB1 is an important non-histone within the nucleus with vital roles during gene transcription, chromatin remodeling, and DNA recombination and repair [16]. The role of HMGB1 in the intervening multiple cellular stressors (e.g. protein aggregates, oxidation, radiation and chemotherapy) may be associated with its subcellular localization and the corresponding biological events it mediates. HMGB1 displacement and release are promoted when the balance of vivo cells in a steady state is disrupted [17]. Intracellular HMGB1 can induce cell proliferation, migration, and invasion, and functions as a prototypic damage-associated molecular pattern (DAMP) molecule that is released from various cancer cells after chemotherapy or radiotherapy and is implicated in many cancer-associated inflammation disorders [17, 18].

Recent evidence demonstrates that HMGB1 plays paradoxical roles in promoting both cancer cell survival and death by regulating multiple signaling pathways, including immunity, genomic stability, proliferation, metastasis, metabolism, apoptosis, autophagy and ferroptosis [18-21]. In neuroblastoma SH-SY5Y cells, endogenous HMGB1-mediated autophagy has been shown to exert a protective effect against oxidative stress-mediated apoptosis by regulating Beclin-1-mediated autophagy [22]. Additionally, exogenous HMGB1-induced autophagy in Schwann cells contributes to neuroblastoma cell proliferation, thus providing a potential therapeutic approach for neuroblastoma development [23]. Our early studies have shown that endogenous HMGB1 acts as a negative regulator of apoptosis and as a positive regulator of autophagy or ferroptosis, playing important roles in leukemia pathogenesis, differentiation and chemotherapy resistance [21, 24-26]. Although the above mentioned studies have succeeded, to a certain extent, in elucidating the role of HMGB1 in the programmed cell death of leukemia cells, its role in the regulation of pyroptosis in neuroblastoma is uncertain.

In this study, we demonstrated that HMGB1 is expressed in neuroblastoma and is associated with clinicopathologic features. As a critical positive regulator of pyroptosis, knockdown of HMGB1 increased DDP/VP16-induced chemosensitivity of SH-SY5Y cells by switching GSDME-mediated pyroptosis to apoptosis. Furthermore, our data suggested a role for endogenous HMGB1 in the regulation of pyroptosis through the ROS/ERK1/2/caspase-3/GSDME pathway, supporting the notion that HMGB1 is a potential drug target for therapeutic interventions in neuroblastoma.

Materials and methods

Reagents and cell culture

Cisplatin (DDP, #S1166), etoposide (VP16, #S1225), N-acetylcysteine (NAC, #S1623), Z-VAD-FMK (#S7023), and U0126-EtOH (#S11-02) were supplied by Selleck (Houston, TX, USA); H₂O₂ (#323381) was obtained from Sigma-Aldrich (St. Louis, MO, USA), EGF (#500-P45) was obtained from Pepro Tech Inc., Rocky Hill, RI, USA). Human T-ALL cell line Jurkat, acute promyelocytic leukemia cell HL-60, and

Endogenous HMGB1 regulates pyroptosis in neuroblastoma cells

Table 1. Relationship between HMGB1 expression and clinical features in neuroblastoma

Clinicopathologic features	Low expression n = 6 (%)	High expression n = 6 (%)	^a P-value
HMGB1	8.8 (6.6-11.3) ^b	15.9 (12-18.8)	0.0022
Age (months)	36.5 (21-118)	56 (29-120)	0.3095
Gender			
Male	4 (66.7%)	4 (66.7%)	> 0.9999
Female	2 (33.3%)	2 (33.3%)	
Tumor Size (cm)			
< 1 cm	3 (50.0%)	1 (16.7%)	0.5455
≥ 1 cm	3 (50.0%)	5 (83.3%)	
Lymph node metastasis			
Yes	4 (66.7%)	5 (83.3%)	> 0.9999
No	2 (33.3%)	1 (16.7%)	
Bone marrow metastasis			
Yes	0 (0%)	6 (100%)	0.0079
No	6 (100%)	0 (0%)	
Clinical stage			
I+II	5 (83.3%)	1 (16.7%)	0.0400
III+IV	1 (16.7%)	5 (83.3%)	
MYCN			
Positive	0 (0%)	5 (83.3%)	0.0152
Negative	6 (100%)	1 (16.7%)	
NSE (μg/L)	33.9 (8.5-59.32)	231.3 (81.7-370)	0.0022
VMA (μmol/d)	18.35 (11-72.8)	112.8 (40.3-189.7)	0.0087
LDH (U/L)	273.5 (224-548)	691.5 (414-1489)	0.0108

HMGB1, High Mobility Group Box 1; NSE, Neuron Specific Enolase; VMA, Vanillylman Acid; LDH, Lactate Dehydrogenase. ^aP-value in Mann-Whitney U test; ^bvalues shown as median minimum-maximum.

chronic myelogenous leukemia cell K562, and human umbilical vein endothelial cells HUVEC, and TPC-1, SH-SY5Y, and 2B cells from Xiangya School of Medicine Type Culture Collection (Changsha, China). HL-60, Jurkat, and K562 cells were cultured in RPMI-1640 medium (GIBCO, Gaithersburg, USA) and TPC-1, HUVEC, SH-SY5Y, and 2B cells in F-12 medium (F12, GIBCO, Gaithersburg, USA) supplemented with 10% heat-inactivated fetal bovine serum (FBS, GIBCO, Gaithersburg, USA) and 1% antibiotics (100 U/mL penicillin G & 100 mg/mL streptomycin) at 37°C in a cell incubator with 5% CO₂ (Thermo Fisher Scientific Inc., USA).

Patients and samples collection

The study protocol was approved by the Ethics Committee of Xiangya Hospital. And written informed consents were obtained from all participants before using clinical samples for researches. Pediatric neuroblastoma and non-tumors tissues (n = 12) were collected from January 2017 to January 2022. The diagnosis,

stage and risk status of neuroblastoma were assessed in accordance with the criteria of National Comprehensive Cancer Network. The general clinical and laboratory profiles of patients were summarized in **Table 1**. Tissue samples were immediately immersed into liquid nitrogen after surgical removal and preserved at -80°C. Frozen tumor tissues and matching normal tissues from 12 cases were subjected to protein extraction for western blot. Samples from 12 patients with complete clinicopathological and clinical information were selected for assessing the correlation of HMGB1 expression with clinical features based on IHC analysis. To detect the expression of HMGB1, collected serum from 5 normal healthy subjects and 12 Pediatric neuroblastoma patients in primary phase and remission phase.

Lentivirus transfection and RNA interference

HMGB1 or GSDME short hairpin RNA (shRNA) lentiviral knockdown and overexpression (Gene-Chem Inc., Shanghai, China) or shRNA non-tar-

Endogenous HMGB1 regulates pyroptosis in neuroblastoma cells

get control (NTC) were packaged with HIV based packaging mix (GeneChem Inc.) for infecting SH-SY5Y cells for establishing cells constitutively repressing HMGB1 or GSDME. Stable clones were selected by puromycin. The HMGB1 shRNA oligonucleotide sequences were as follows: HMGB1 shRNA1: 5'-CCGGGATGCAGCTT-ATACGAAATAACTCGAGTTATTTTCGTATAAGCTGC-ATCTTTTTG-3'; HMGB1 shRNA2: 5'-CCGGTCG-GGAGGAGCATAAGAAGAACTCGAGTTCTTCTTAT-GCTCCTCCCGATTTTTG-3'; HMGB1 shRNA3: 5'-CCGGTTCTCTTCTGCTCTGAGTATCTCGAGATAC-CAGAGCAGAAGAGGAATTTTT-3'.

The GSDME shRNA oligonucleotide sequences were as follows: GSDME shRNA1: 5'-CCGGGC-ATGATGAATGACCTGACTTCTCGAGAAGTCAGG-TCATTCATCATGCTTTTTG-3'; GSDME shRNA2: 5'-CCGGGCGGTCTATTTGATGATGAACTCGAGT-TCATCATCAAATAGGACCGCTTTTTG-3'; GSDME shRNA3: 5'-CCGGGCATTCATAGACATGCCAGATC-TCGAGATCTGGCATGTCTATGAATGCTTTTTG-3'. Non-silencing shRNA (control shRNA) were used as mock-transfected controls (target sequence: TTCTCCGAACGTGTACAGT). Then HMGB1 or GSDME expression was verified by qRT-PCR and western blot. Two of GSDME shRNA (GSDME shRNA1 and GSDME shRNA2) that proved the most effective for knockdown of gene expression were selected. GSDME shRNA1 and GSDME shRNA2 was also performed in this study (Figure S1A and S1D). Also, HMGB1 shRNA1 was proved the most effective for knockdown of gene expression were selected, which was performed in this study (Figure S1B and S1E). Overexpression HMGB1 vector were used according to the manufacturer's instructions, it overexpression was verified by qRT-PCR and western blot (Figure S1C and S1F).

Quantitative real-time PCR (qRT-PCR)

Trizol reagent (Invitrogen, USA) according to the manufacturer's instructions and cDNA synthesis via PrimeScript™ RT master mix (Yeasen Biotech Co., Ltd., Shanghai, China). A 7900 Real-Time PCR System (Applied Biosystems, Foster City, CA) with Hieff® qPCR SYBR Green Master Mix (Low Rox Plus Yeasen Biotech Co., Ltd., Shanghai, China) was used for performing quantitative PCR (qPCR). Relative mRNA expression was standardized using the house-keeping gene β -actin forward (5'-TCCTTCCTGG-GCATGGAGTC-3') and reverse (5'-GTAACGCAA-CTAAGTCATAGTC-3'). The following human prim-

ers were used in this study: HMGB1 forward (5'-TTTCAAACAAAGATGCCACA-3') and reverse (5'-GTTCCCTAAACTCCTAAGCAGATA-3'); GSDME forward (5'-TGCCTACGGTGCATTGAGTT-3') and reverse (5'-TCTGGCATGTCTATGAATGCAAA-3'). Cycling conditions were as follows: 95°C for 5 min, followed by 40 cycles of 95°C for 10 s, 60°C for 30 s. The relative gene expressions were calculated by the $2^{-\Delta\Delta Ct}$ method. Samples were examined in triplicate.

Antibodies, preparation of subcellular fractions and western blot

The following commercially available antibodies were used: GSDME (#ab215191) were obtained from Abcam, HMGB1 antibodies (#A1-9529), Caspase-3 (#A0214) and cleaved caspase-3 (#A11021), Actin antibodies (#AC026) were obtained from abclonal (Wuhan, China). p-ERK1/2 (#R24245), total ERK1/2 (#R22685) and PARP (#R25279) antibodies were obtained from Zhengneng (Chengdu, China). Horseradish peroxidase (HRP)-conjugated goat anti-rabbit IgG (#AS014) from ABclonal (Wuhan, China); Cells were rinsed with PBS, collected and resuspended in lytic buffer (Beyotime, Beijing, China) and maintained on ice for 15 min. Cytosolic/nuclear extracts and total cellular lysates were prepared using the NE-PER nuclear and cytoplasmic extraction kit (Pierce, Rockford, USA) according to the manufacturer's instructions. Protein concentrations of the extracts were measured with BCA assay (Pierce, Rockford, USA) and equalized with the extraction reagents. Whole cell lysates were separated by 10% or 12% sodium dodecyl sulfate-polyacrylamide gel electrophoresis (SDS-PAGE) and subsequently electrophoretically transferred onto polyvinylidene difluoride (PVDF) blotting membranes (Millipore, USA). The membranes were blocked with 5% non-fat dry milk in Tris-buffered saline containing Tween 20 (TBST; 50 mM Tris [pH 7.5], 100 mM NaCl, 0.15% Tween-20), incubated with diluted primary antibodies for 12 h at 4°C, and rinsed thrice with TBST for 10 min. Then the membranes were incubated with different secondary antibodies for 12 h at 4°C and hybridization was detected by enhanced chemiluminescent reagents (Zen-Bioscience, Chengdu, China) after rinsing thrice with TBST for 10 min. Membranes were exposed to radiographic film and the expression levels of targeted proteins quantified. A BIO-RAD ChemiDoc™ MP Imaging

Endogenous HMGB1 regulates pyroptosis in neuroblastoma cells

System was employed for quantifying and analyzing specific bands via western blot.

Cell viability assay

Cell viability was evaluated using a cell counting kit-8 (CCK-8; #K1018, APE x BIO Technology LLC, USA) according to the manufacturer's instructions. Briefly, cells (5×10^4 /well/100 μ L) were seeded into a 96-well plate and treated with different drugs at various concentrations for the indicated times. After the addition of 10 μ L of CCK-8 solution to each well, cells were incubated at 37°C for another 3 h and the absorbance was determined at 450 nm using a microplate reader. All experiments were performed in triplicate.

Measurements of HMGB1 release

Supernatants from different treatments of SH-SY5Y cells were collected and used to determine the concentration of HMGB1. Serum from different groups of patients and normal subjects were collected and used to determine the concentration of HMGB1. The release of HMGB1 into supernatants was evaluated with enzyme-linked immunosorbent assay (ELISA) kits from Enzyme-linked Biotechnology Co., Ltd. (Shanghai, China) according to the manufacturer's instructions. All experiments were performed in triplicate.

LDH release assay

The LDH release assay was performed following the manufacturer's protocols. The total LDH present in the culture medium from the control group was set as 100%, and LDH release was calculated as follows: LDH release (%) = (OD of the drug-treated group - OD of blank control group)/(OD of the maximum group - OD of blank control group) \times 100%. Lactate dehydrogenase (LDH) assay kit was obtained from Nanjing Jiancheng Bioengineering Institute.

Immunofluorescent analysis

Cells were fixed in 4% formaldehyde for 30 min at room temperature prior to cell permeabilization with 0.1% Triton X-100 (4°C, 10 min). After saturating with PBS containing 2% bovine serum albumin for 1 h at room temperature, the samples were processed for immunofluorescence with HMGB1 antibodies (#A19529) followed by Alexa Fluor 488-conjugated immu-

noglobulin and DAPI (Beyotime, Beijing, China). Between all incubation steps, cells were rinsed thrice for 3 min with PBS containing 0.2% bovine serum albumin. Fluorescent signals were analyzed using Leica TCS SP8 fluorescence microscope.

DNA fragmentation evaluation

DNA fragmentation of endothelial cells was measured by TUNEL staining assay as previously described. Briefly, endothelial cells were cultured on cover slips in a 24-well plate. After the indicated treatments, the cells were fixed with 4% paraformaldehyde and permeabilized with 0.3% Triton X-100. After washing with PBS, cells were incubated with TUNEL reaction mixture at 37°C in the dark for 1 h, and stained by DAPI. Then the results were visualized by a fluorescence microscope (Nikon, A1 PLUS, Tokyo, Japan).

Immunohistochemistry

Both patient samples and murine tumors were fixed in 10% formalin for 24 h. After dehydration and paraffin embedding, the specimens were sliced into 5 μ m thick sections by a microtome (Leica, Wetzlar, Germany) and mounted on glass slides. The expressions of cleaved caspase-3, p-ERK, and PARP were measured by immunostaining. After deparaffinization and rehydration, the sections were pressure-cooked for 2 min in an antigen retrieval buffer (0.01 M citrate buffer, pH 6.0) for unmasking antigens. Then the sections were incubated with anti-rabbit cleaved caspase-3, p-ERK and cleaved-PARP monoclonal antibodies at 4°C overnight respectively, followed by biotinylated goat anti-rabbit IgG (1:100, No. IB-0021, Dingguo, Beijing, China) secondary antibody (ZSGB-bio, Beijing, China) for 1 h at 37°C and streptavidin-HRP.

Reactive oxygen species (ROS) measurement

The ROS levels in SH-SY5Y cells were detected with the Reactive Oxygen Species Assay Kit (No. C1300, Applygen, Beijing, China). After different treatments, the SH-SY5Y cells were washed with PBS and stained with DHE (10 μ M) for 30 min at 37°C in the dark. Then, the DHE fluorescence of cells was detected using a fluorescence trophotometer at an excitation wavelength of 535 nm and an emission wavelength

Endogenous HMGB1 regulates pyroptosis in neuroblastoma cells

of 610 nm. The incremental production of ROS was expressed as a percentage of the control.

Tumor cell xenograft model

Sixteen specific pathogen-free-grade male BALB/c nude mice (4-6 weeks of age) were purchased from Xiangya Medical College Animal Laboratory (Changsha, China). All experiments were approved by the Animal Ethics Committee of Xiangya Medical College, Central South University, China. The animals were raised in pathogen-free conditions with a 12 hour light-dark cycle with water and food provided ad libitum. For each experiment, 16 mice were randomly divided into the following four groups: (1) control shRNA model receiving PBS (vehicle); (2) control shRNA model receiving DDP; (3) HMGB1 shRNA model receiving PBS (vehicle) and (4) HMGB1 shRNA model receiving DPP. Indicated SH-SY5Y cells were subcutaneously injected into the dorsal flanks right of the midline in nude mice (weight, approximately 20 g). After 4 weeks, tumors reached 100 mm³ in volume recorded, mice were intraperitoneal injected with DDP (2 mg/kg, i.p., every three days) for three weeks. The tumor volume (length × width² × π/6) and body weight of the mice were monitored every three days. At the end of treatment, mice were sacrificed and the tumors were removed, weighted, and analyzed via IHC and western blot.

Statistical analysis

Statistical analysis each experiment is repeated at least three times independently. Data are presented as means ± standard deviations. Quantitative results were analyzed using GraphPad Prism 7 (GraphPad Software Inc., San Diego, CA, USA). Comparisons between two groups were made using two-tailed Student's t-tests. The relationship between HMGB1 expression and clinicopathologic features was analyzed through the Mann-Whitney test. $P < 0.05$ was considered to indicate statistical significance.

Results

HMGB1 expression is upregulated in neuroblastoma and associated with clinicopathologic features

We first determined the level of HMGB1 expression in SH-SY5Y cells by qRT-PCR and western blotting. Similar to the leukemia (HL-60, K562

and Jurkat) and thyroid cancer cell line TPC-1 in our previous studies [25-27], HMGB1 expression was high in SH-SY5Y cells but low in 2B and human umbilical vein endothelial cells (**Figure 1A** and **1B**). To further determine the role of HMGB1 in neuroblastoma progression, we initially evaluated HMGB1 expression in 12 neuroblastoma specimens. Both western blot and immunohistochemistry revealed that HMGB1 protein expression was significantly higher in tumors compared to non-tumor tissues (**Figure 1C** and **1D**). We also found upregulated HMGB1 expression in serum derived from patients with primary neuroblastoma. Conversely, these levels were lower in serum derived from normal healthy subjects or patients who demonstrated complete remission (**Figure 1E**). Thus, HMGB1 may play an important role in tumorigenesis.

We next investigated the relationship between the relative expression of HMGB1 and clinical features. Based on 12 neuroblastoma tissues, the patients were classified into low- and high-expression groups according to the median value. The results indicated that later clinical-stage, bone marrow metastasis, MYCN gene, NSE, VMA, and LDH levels were significantly correlated with high HMGB1 expression (**Table 1**). However, no significant association existed between HMGB1 expression and sex, age, or lymph node metastasis (**Table 1**). Thus, HMGB1 reflected different clinicopathologic features in pediatric neuroblastoma.

DDP/VP16-induced pyroptosis is required for HMGB1 translocation and release

Chemotherapy drugs that activate caspase-3, such as topotecan, VP16, DDP, and CPT-11, induce pyroptotic cell death in SH-SY5Y cells, which are sensitive to the caspase-3 inhibitor Z-VAD-FMK [11]. HMGB1 protein is both a nuclear DNA binding factor and a secreted protein, the activities of which are determined by its intracellular localization and posttranslational modifications [16, 27]. To evaluate whether HMGB1 translocation and extracellular release was regulated by DDP/VP16-induced pyroptosis, we detected the HMGB1 protein levels and immunofluorescence staining in SH-SY5Y cells pretreated with Z-VAD-FMK and shGSDME. We found that HMGB1 was located in the nucleus and cytosol, but was higher in the cytosol under DDP or VP16 treatment. Pretreatment of Z-VAD-FMK for 3 h in SH-SY5Y

Endogenous HMGB1 regulates pyroptosis in neuroblastoma cells

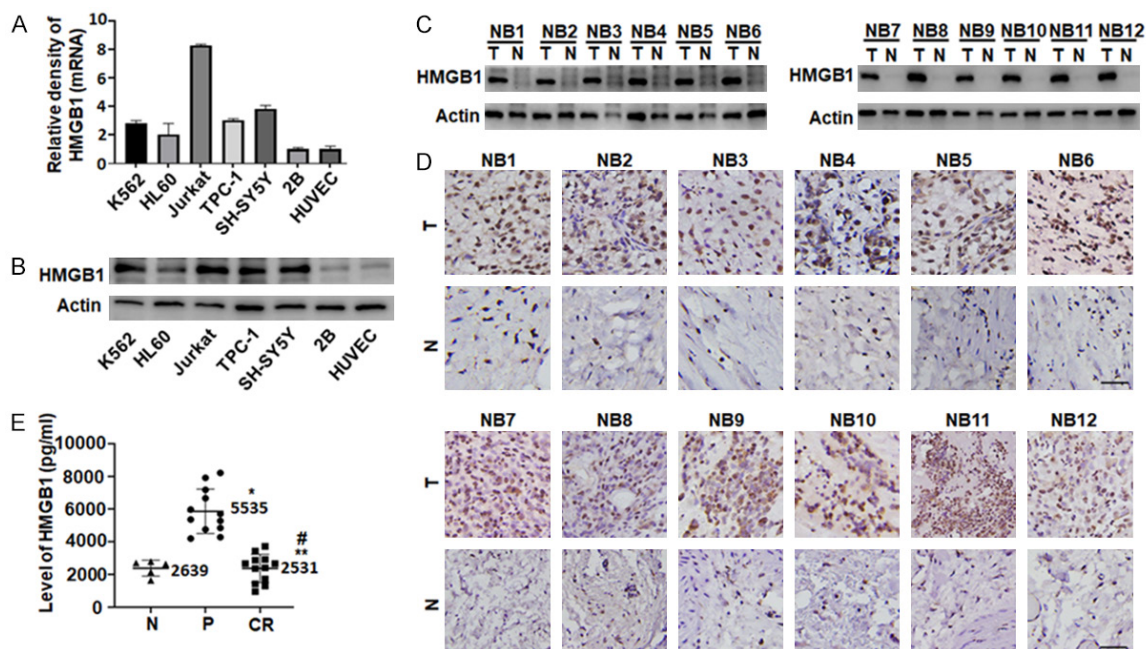


Figure 1. HMGB1 expression is up-regulated in neuroblastoma and associated with clinicopathologic features. A and B. QRT-PCR and western blot of HMGB1 and actin in various cell lines hinted at an over-expression of HMGB1 in SH-SY5Y cell lines; C and D. Western blot and IHC analysis showed that HMGB1 expression was higher in tumors than non-tumors. T, tumor; N, non-tumor; Scale bars, 100 μ m; E. Expression of HMGB1 in serum of different patients and normal healthy subjects. N, normal healthy subject; P, primary; CR, complete remission; * $P < 0.05$ vs. normal subject; ** $P > 0.05$ vs. normal subject; # $P < 0.05$ vs. primary.

cells reduced HMGB1 expression in the cytosol, indicating that Z-VAD-FMK inhibited pyroptosis blocked HMGB1 translocation from nucleus into the cytosol (Figures 2A and 2B, S2A and S2B). Consistent with this finding, knockdown of GSDME expression also blocked HMGB1 translocation (Figures 2A and 2B, S2A and S2B). Furthermore, pretreatment with Z-VAD-FMK or GSDME depletion inhibited HMGB1 release into supernatants incubated with DDP or VP16 (Figures 2C, S2C). The overall results suggests that DDP/VP16-induced pyroptosis is required for HMGB1 translocation and release in SH-SY5Y cells.

Depletion of HMGB1 inhibits DDP/VP16-induced pyroptosis

We have previously demonstrated that chemotherapeutic drugs-induced pyroptosis promoted HMGB1 cytosolic translocation and extracellular release in SH-SY5Y cells (Figure 2), suggested that HMGB1 played an important role in the pathophysiological processes of DDP/VP16-induced pyroptosis. However, the role of HMGB1 in regulating pyroptosis remains unclear. The typical characteristics of pyroptosis, include the large bubbled morphology, the

generation of GSDME-N terminal (GSDME-NT) fragments, and the release of LDH. To explore the potential role of HMGB1 in the regulation of pyroptosis, a target-specific shRNA against HMGB1 was transfected into SH-SY5Y cells. Knockdown of HMGB1 significantly decreased DDP or VP16-induced GSDME-NT and cleaved caspase-3 expression compared to that observed in the control group (Figure 3A). Moreover, DDP or VP16 dose-dependently increased LDH release in SH-SY5Y cells, whereas knockdown of HMGB1 expression significantly decreased LDH release compared to the control group (Figure 3B). Finally, ultrastructural analysis provided the most convincing evidence of pyroptosis. After a depletion of HMGB1, SH-SY5Y cells exhibited less bubbled morphology compared to the control shRNA group (Figure 3C), supporting the critical role of HMGB1 in regulating pyroptosis.

Depletion of HMGB1 switches DDP/VP16-induced cell death from pyroptosis to apoptosis

Mounting evidence has indicated that apoptosis plays an important role in the regulation of cancer development and progression and in

Endogenous HMGB1 regulates pyroptosis in neuroblastoma cells

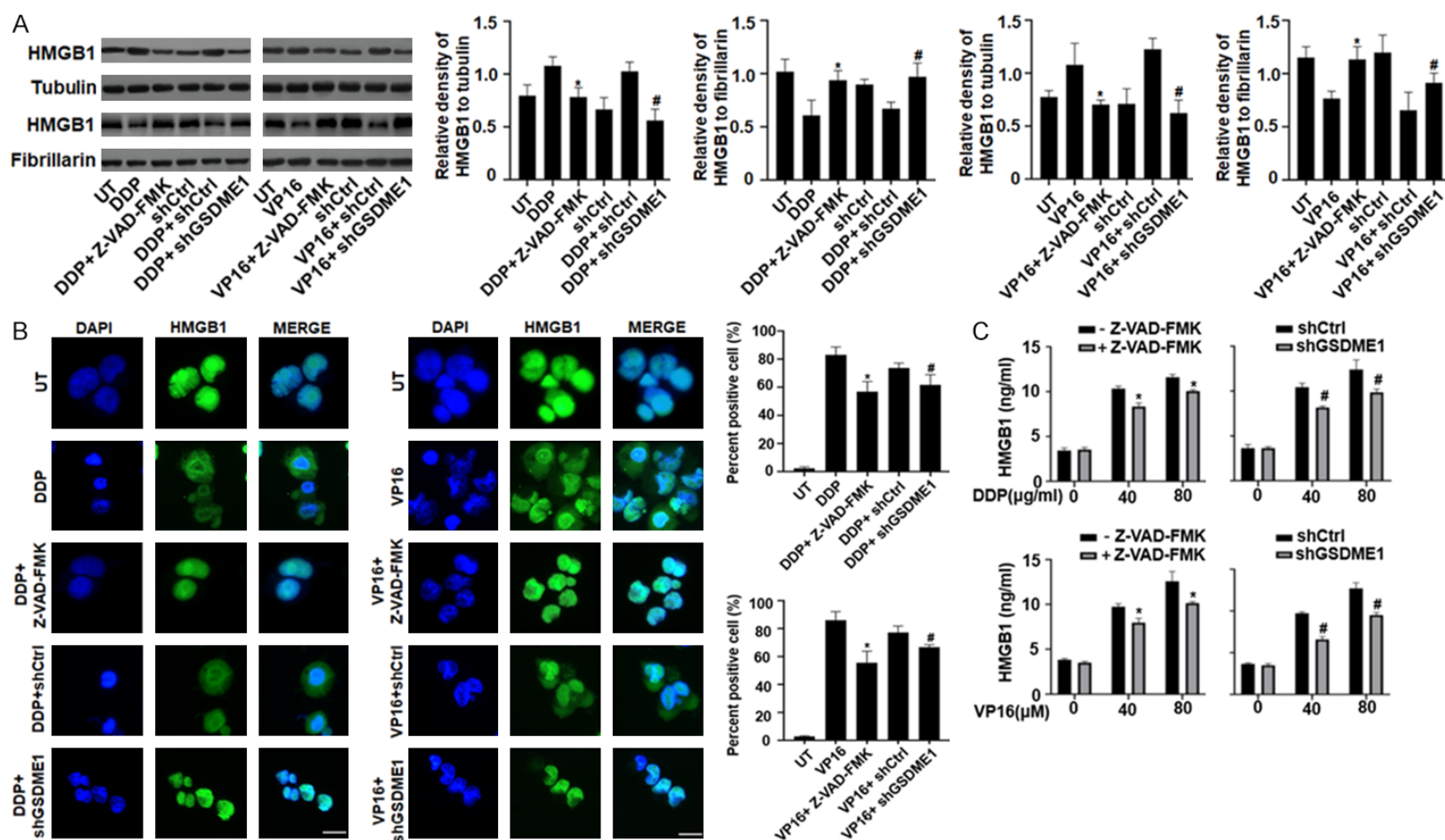


Figure 2. DDP/VP16-induced pyroptosis is required for HMGB1 translocation and release. A and B. SH-SY5Y cells were transfected with GSDME1 shRNA and control shRNA, or pretreated with or without Z-VAD-FMK (10 µM) for 24 h, and then treated with DDP (40 µg/ml) and VP16 (40 µM) for 24 h, respectively. The nuclear/cytoplasmic HMGB1 protein expression was assayed by western blot and immunofluorescence (Green, HMGB1; blue, nucleus). Scale bars, 100 µm; (n = 3, *P < 0.05 vs. DDP or VP16 treatment group; #P < 0.05 vs. DDP or VP16+shCtrl group). C. SH-SY5Y cells were transfected with GSDME1 shRNA and control shRNA, or pretreated with or without Z-VAD-FMK (10 µM) for 24 h, and then treated with DDP and VP16 at the indicated doses for 24 h, respectively. The release of HMGB1 was analyzed by ELISA (n = 3, *P < 0.05 vs. Z-VAD-FMK treatment group; #P < 0.05 vs. shCtrl group).

Endogenous HMGB1 regulates pyroptosis in neuroblastoma cells

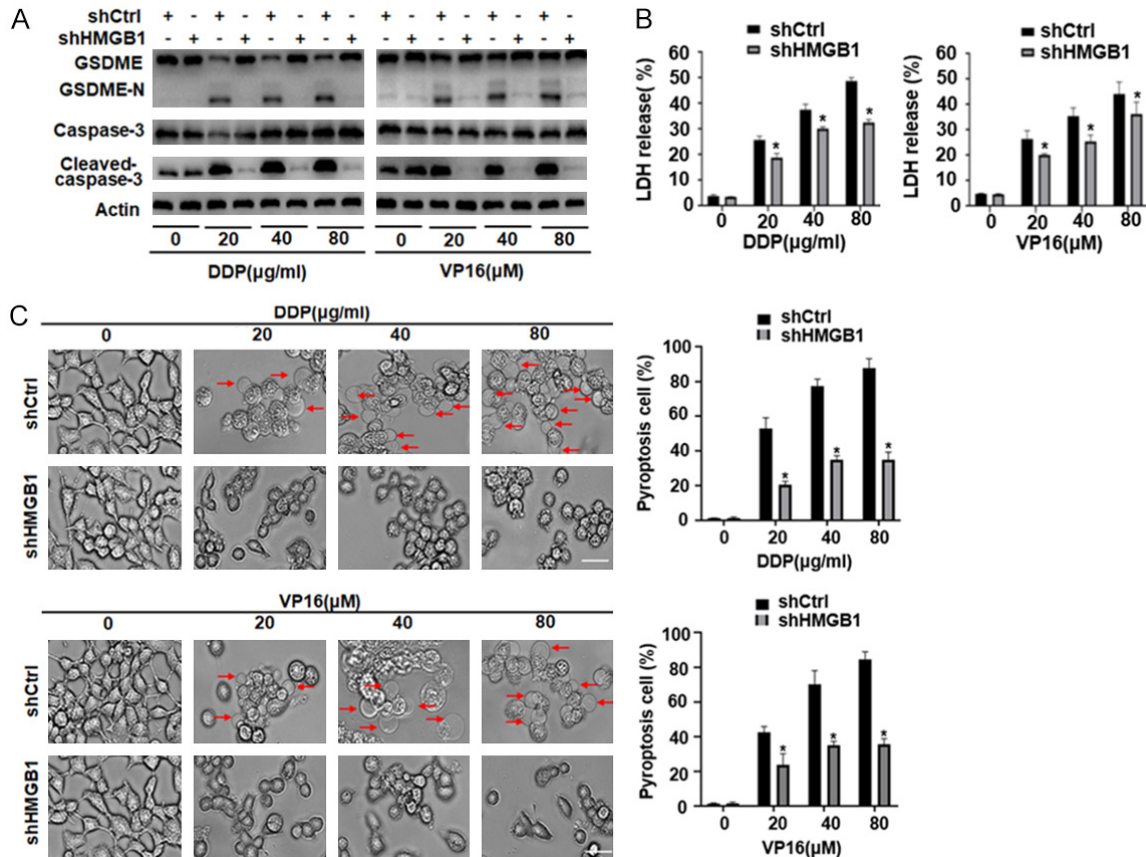


Figure 3. Depletion of HMGB1 inhibits DDP/VP16-induced pyroptosis. A and B. SH-SY5Y cells were transfected with HMGB1 shRNA and control shRNA and then treated with DDP and VP16 at the indicated doses for 24 h, respectively. GSDME-N and cleaved caspase-3 levels were assayed by western blot. LDH-release was analyzed using LDH assay kit and expressed as mean \pm SD ($n = 3$, $^*P < 0.05$ vs. shCtrl group). C. Representative light microscopy images of SH-SY5Y cells with differently treatments were detected. The red arrow indicates bubbles emerging from the plasma membrane ($n = 3$, $^*P < 0.05$ vs. shCtrl group).

determining the response of tumor cells to anticancer therapy [28]. Chemotherapeutic drugs that activate caspase-3 were subsequently shown to induce pyroptotic cell death in cell lines expressing high levels of GSDME, whereas they induced apoptosis in GSDME-negative cells [11]. Moreover, we found that endogenous HMGB1 is a positive regulator of pyroptosis in SH-SY5Y cells (Figure 3). To determine whether HMGB1-regulated GSDME expression affected chemosensitivity and apoptosis in DDP/VP16-treated SH-SY5Y cells, we first examined cell viability using the CCK-8 assay. DDP or VP16 dose-dependently induced growth inhibition in SH-SY5Y cells, whereas the depletion of HMGB1 expression significantly increased the chemosensitivity compared to that of the control group (Figure 4A). Moreover, depletion of HMGB1 expression increased

in the anticancer drug-induced apoptosis, as indicated by increases in TUNEL staining and cleavage of PARP, but not cleaved caspase-3 (Figure 4B and 4C). In contrast, up-regulated HMGB1 expression significantly decreased DDP or VP16-induced cleavage of PARP expression (Figure S3A). These data suggested that knocking out HMGB1 switched DDP/VP16-induced cell death from pyroptosis to apoptosis.

Endogenous HMGB1 regulates DDP/VP16-induced pyroptosis in the ROS-ERK1/2 pathway

ROS function as signaling molecules regulating both cell survival and death through various pathways. Elevated ROS stimulate caspase-3/GSDME-dependent pyroptosis in cancer cells

Endogenous HMGB1 regulates pyroptosis in neuroblastoma cells

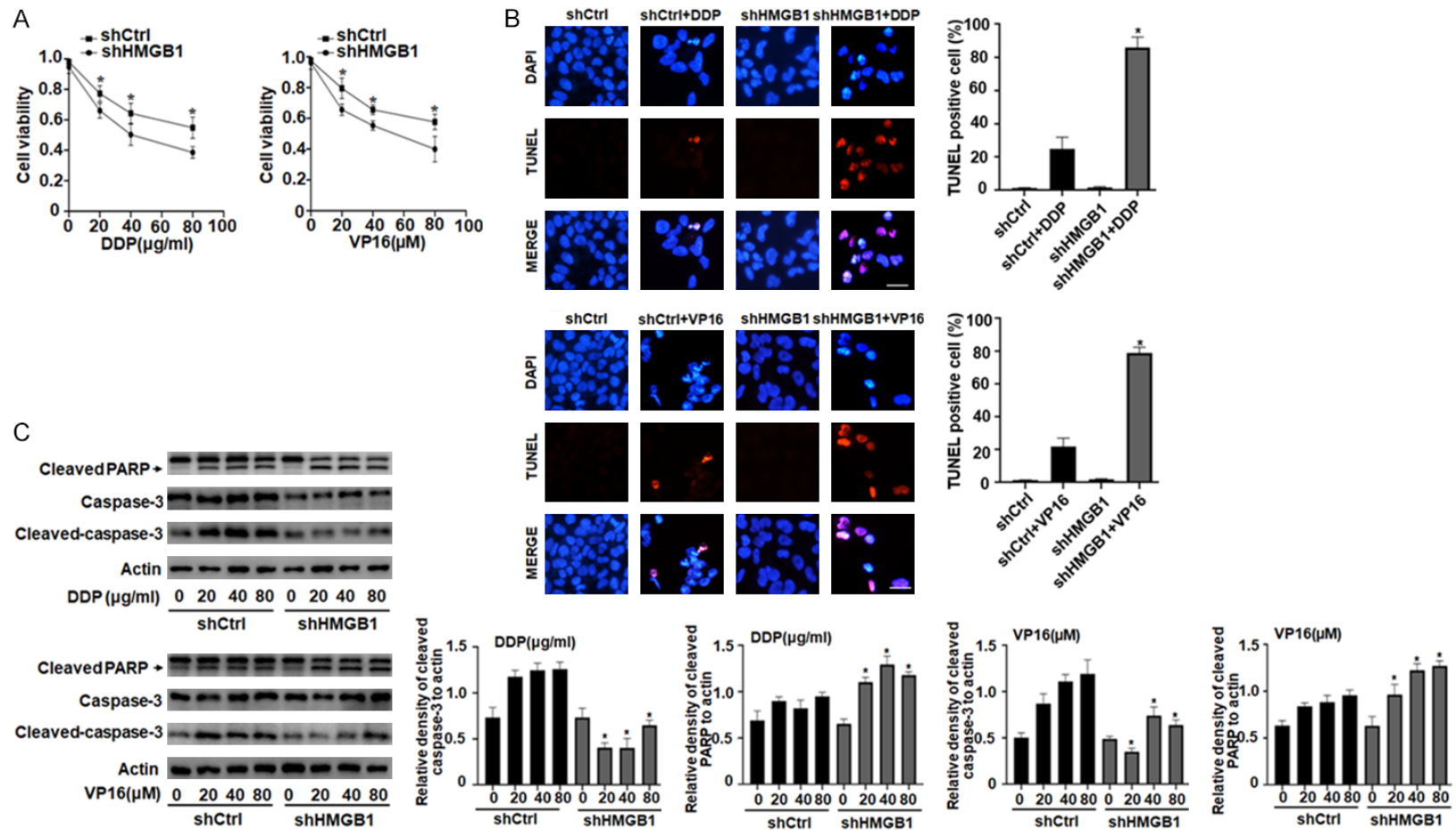


Figure 4. Depletion of HMGB1 switches DDP/VP16-induced cell death from pyroptosis to apoptosis. **A.** SH-SY5Y cells were transfected with HMGB1 shRNA and control shRNA and then treated with DDP and VP16 at the indicated doses for 24 h, respectively. Cell viability was assayed using a CCK-8 kit ($n = 3$, $^*P < 0.05$ vs. shHMGB1 group). **B.** SH-SY5Y cells were transfected with HMGB1 shRNA and control shRNA and then treated with DDP (40 $\mu\text{g/ml}$) and VP16 (40 μM) for 24 h, respectively. Apoptosis was determined using TUNEL assay in the four groups. Red fluorescence indicates TUNEL-positive cells in the microscopic fields. Scale bars, 100 μm ($n = 3$, $^*P < 0.05$ vs. shCtrl+DDP or VP16 group). **C.** SH-SY5Y cells were transfected with HMGB1 shRNA and control shRNA and then treated with DDP and VP16 at the indicated doses for 24 h, respectively. Cleaved PARP and cleaved caspase-3 levels were assayed by western blot ($n = 3$, $^*P < 0.05$ vs. shCtrl group at the indicated doses respectively).

Endogenous HMGB1 regulates pyroptosis in neuroblastoma cells

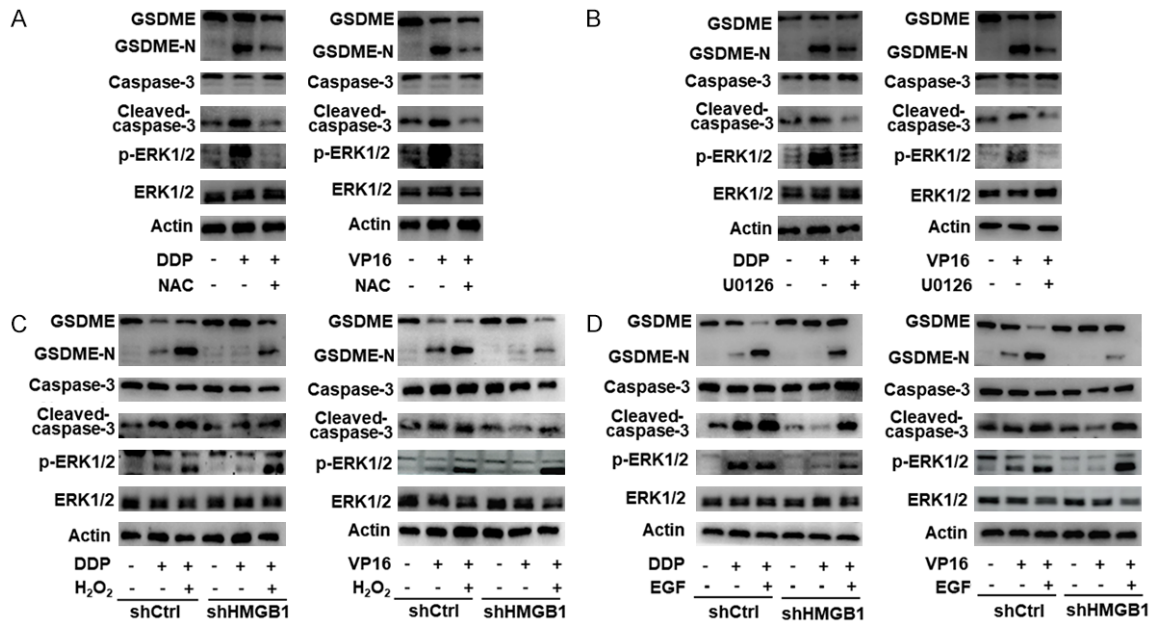


Figure 5. Endogenous HMGB1 regulates DDP/VP16-induced pyroptosis in a ROS-ERK1/2 pathway. **A.** SH-SY5Y cells were pretreated with or without NAC (20 μ M) for 12 h, and then treated with DDP (40 μ g/ml) and VP16 (40 μ M) for 24 h, respectively. GSDME-NT, cleaved caspase-3 and p-ERK1/2 levels were assayed by western blot. **B.** SH-SY5Y cells were pretreated with or without U0126 (10 μ M) for 12 h, and then treated with DDP (40 μ g/ml) and VP16 (40 μ M) for 24 h, respectively. GSDME-NT, cleaved caspase-3 and p-ERK1/2 levels were assayed by western blot. **C.** SH-SY5Y cells were transfected with HMGB1 shRNA and control shRNA, with or without H₂O₂ (50 μ M) for 48 h, and then treated with DDP (40 μ g/ml) and VP16 (40 μ M) for 24 h, respectively. GSDME-NT, cleaved caspase-3 and p-ERK1/2 levels were assayed by western blot. **D.** SH-SY5Y cells were transfected with HMGB1 shRNA and control shRNA, or pretreated with or without EGF (50 ng/ml) for 48 h, and then treated with DDP (40 μ g/ml) and VP16 (40 μ M) for 24 h, respectively. GSDME-NT, cleaved caspase-3 and p-ERK1/2 levels were assayed by western blot.

[15, 29]. The ERK1/2 pathway is involved in many cellular processes, including cell proliferation, chemoresistance, survival, and death, and reportedly plays pivotal roles in caspase-3 activation, which contributes to GSDME-dependent pyroptosis [30, 31]. However, whether the ROS/ERK1/2 signaling pathway by which pyroptosis is induced in response to HMGB1 was previously unclear. To determine the role of ROS in regulating chemotherapeutic drug-induced pyroptosis, we first examined whether DDP or VP16 induced ROS production in SH-SY5Y cells. The results showed that treatment with DDP or VP16 induced ROS production, whereas pretreatment with the ROS quencher NAC decreased ROS production (Figure S4A). Moreover, co-treatment with NAC and DDP or VP16 for 24 h inhibited chemotherapeutic drug-induced GSDME-NT, cleaved caspase-3, and ERK1/2 phosphorylation (p-ERK1/2) expression compared to the DDP or VP16 alone group (Figure 5A). These results indicated that the ERK1/2 pathway may be a downstream signal of ROS. Furthermore, pre-

treatment with the MEK inhibitor U0126 also inhibited chemotherapeutic drug-induced GSDME-NT and cleaved caspase-3 expression but did not affect ROS production (Figures 5B, S4B), suggesting that chemotherapeutic drugs promote pyroptosis through the ROS/ERK1/2/caspase-3/GSDME pathway.

To further characterize the role of the ROS/ERK1/2/caspase-3/GSDME pathway in HMGB1-mediated pyroptosis, we treated cells with DDP or VP16 and the ROS agonist H₂O₂ and the ERK agonist EGF. We found that depletion of HMGB1 expression significantly decreased ROS production, GSDME-NT, cleaved caspase-3, and p-ERK1/2 expression compared with the control group (Figures 5C, S4C). Moreover, we found that up-regulated HMGB1 promotes ROS production (Figure S4D). Pretreatment of H₂O₂ or EGF reversed the HMGB1 depletion-induced decrease in GSDME-NT, cleaved caspase-3, and p-ERK1/2 expression relative to the DDP or VP16 alone group (Figure 5C and 5D). In contrast, up-regulated HMGB1 expres-

Endogenous HMGB1 regulates pyroptosis in neuroblastoma cells

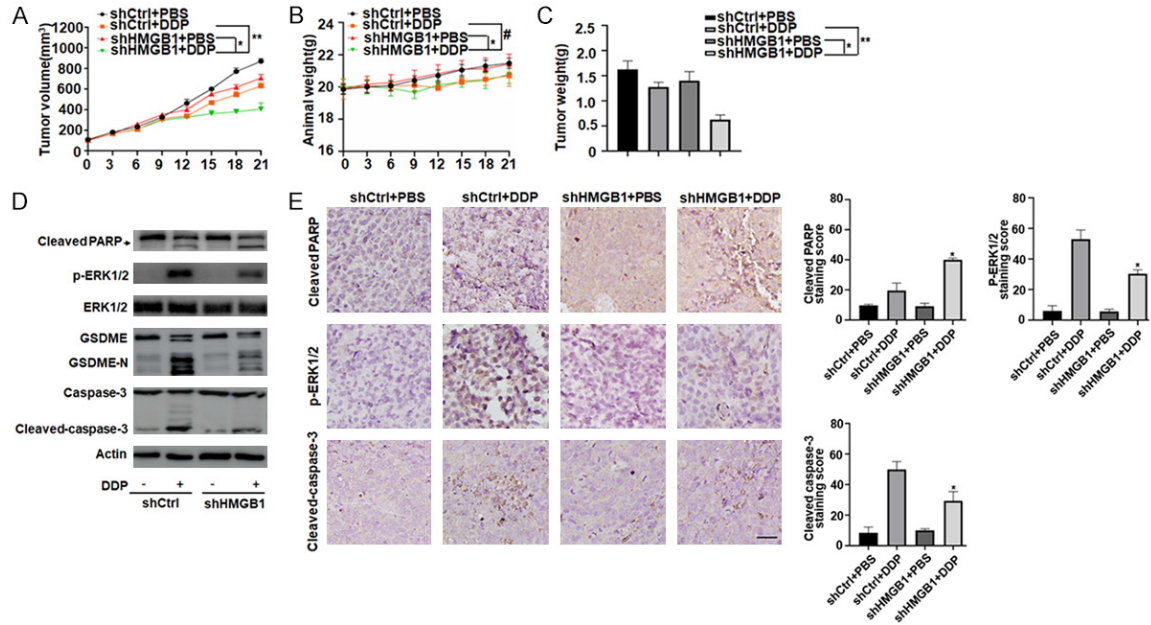


Figure 6. Knockdown of HMGB1 expression inhibits DDP-induced pyroptosis in vivo. A-C. BALB/c nude mice were injected subcutaneously with HMGB1 shRNA SH-SY5Y cells (1×10^7 cells/mouse). After 4 weeks, DDP (2 mg/kg, every three days) were intraperitoneally injected into the mice for 3 weeks. Tumor volumes and animal weight were measured every three days. At the termination of the experiments, all xenografts were removed and weighted ($n = 4$ mice/group, $*P < 0.05$, $**P > 0.05$, $\#P > 0.05$). D. Western blot analysis of cleaved PARP, GSDME-NT, cleaved caspase-3 and p-ERK1/2 expressions were performed with an isolated tumor at the termination of the experiments. All experiments were conducted in triplicate. E. Immunohistochemical staining of cleaved PARP, cleaved caspase-3 and p-ERK1/2 were performed with an isolated tumor at the termination of the experiments. All experiments were conducted in triplicate. Scale bars, 100 μm . ($n = 3$, $*P < 0.05$ vs. shCtrl+DDP group).

sion significantly increased DDP or VP16-induced GSDME-NT and cleaved caspase-3 expression, LDH release and exhibited more bubbled morphology compared to the vector group (Figure S3A, S3B and S3C). Furthermore, pretreatment with ROS inhibitor (NAC) or MEK inhibitor (U0126) reversed the HMGB1 overexpression-induced increase in GSDME-NT, cleaved caspase-3, and p-REK1/2 expression relative to the DDP or VP16 alone group (Figure S3D and S3E). Collectively, these data indicate that HMGB1 regulated DDP/VP16-induced pyroptosis through the ROS/ERK1/2/caspase-3/GSDME pathway.

Knockdown of HMGB1 expression inhibits DDP-induced pyroptosis in vivo

To investigate whether the suppression of HMGB1 expression affected DDP-induced pyroptosis in vivo, stable HMGB1-knockdown SH-SY5Y cells were subcutaneously introduced into the right flank of nude mice. Four weeks post-injection, we treated nude mice with DDP (2 mg/kg) or PBS via intraperitoneal injection.

Compared to the control shRNA group, DDP treatment effectively reduced the size of tumors formed by HMGB1-knockdown cells. The average tumor volume in mice injected with HMGB1 shRNA SH-SY5Y was smaller than that in mice injected with the control shRNA SH-SY5Y cells at all time points (Figure 6A). Notably, the body weight of mice did not significantly differ between groups with or without HMGB1 depletion (Figure 6B). At the end of the experiments, the weights of the xenografts formed by HMGB1-knockdown cells were reduced compared to those of control shRNA mice (Figure 6C), indicating that these HMGB1-knockdown cells are more sensitive to the DDP chemotherapy regimen. These results indicate that these HMGB1-knockdown cells formed tumors that increased the sensitivity of the chemotherapeutic agents.

Based on western blotting the expression of GSDME-N, a marker for the assessment of pyroptosis in vivo, indicated that knockdown of HMGB1 decreased DDP-induced GSDME-N expression and pyroptosis. Meanwhile, cleaved-

Endogenous HMGB1 regulates pyroptosis in neuroblastoma cells

caspace-3 and p-ERK1/2 were also inhibited in the HMGB1 shRNA group compared to control shRNA group (Figure 6D). In contrast, knock-down of HMGB1 significantly increased DDP-induced cleaved-PARP expression and apoptosis (Figure 6D). Consistently, immunohistochemistry analysis revealed that cleaved-caspase-3 and p-ERK1/2, but not cleaved-PARP, were also weakly expressed in tumors formed by HMGB1-knockdown cells (Figure 6E). Therefore, we deduced that HMGB1 regulated DDP-induced pyroptosis through the ERK1/2/caspase-3/GSDME signaling pathway *in vivo*.

Discussion

Recently, several studies have focused on elucidating the molecular mechanism underlying pyroptosis as well as the mechanism that induces pyroptosis in tumor cells. It is emerging as a potential mechanism for targeting tumor growth due to its ability to potentiate cell death in some malignancies. In the this study, we demonstrated that a novel function of HMGB1 was direct involvement in the positive regulation and maintenance of pyroptosis in DDP/VP16-treated SH-SY5Y cells, possibly through regulating caspase-3 and GSDME activation. Depletion of HMGB1 inhibited DDP/VP16-induced pyroptosis and increased the chemosensitivity and apoptosis of SH-SY5Y cells *in vitro* and *in vivo* through a ROS/ERK1/2-dependent pathway. Therefore, our findings may provide novel treatment options for patients with neuroblastoma.

The HMGB1 protein is both a nuclear DNA binding factor and a secreted protein which plays complex roles in various biological processes and in the development of many diseases, including autoimmune diseases and cancer. Overexpression of HMGB1 has been demonstrated in numerous types of cancer, including breast cancer, colorectal cancer, lung cancer, and hepatocellular carcinoma. Our early studies have shown that HMGB1 was expressed abundantly in leukemia and thyroid cancer, and positively correlated with clinical status of patients [26]. However, the role of HMGB1 in childhood neuroblastoma is not yet clearly defined. In this study, we found that HMGB1 expression was upregulated in SH-SY5Y cells and in samples derived from patients with neuroblastoma. Moreover, the expression levels were correlated with the clinicopathological

features of patients with neuroblastoma. Higher related to later clinical stage, bone marrow metastasis, MYCN gene, and NSE, VMA, and LDH levels, suggesting a potential contributory role of HMGB1 in tumorigenesis of neuroblastoma.

Neuroblastoma is the most common cancer in infants and one of the most common extracranial solid tumors in children younger than 5 years. The main causes of death in patients with neuroblastoma include metastasis (present in up to 70% of patients at the time of diagnosis) and tumor resistance to conventional treatment [1, 2]. DDP-based chemotherapy is a major regimen to treat neuroblastoma, but its clinical efficacy is limited by chemoresistance [2, 3]. Pyroptosis, a novel form of programmed cell death, has recently been reported to play significant role in the modulation of cancer progression and is considered a promising strategy for cancer treatment [8]. Numerous studies have demonstrated that chemotherapy drug (Topotecan, VP16, DDP or CPT-11)-induced pyroptosis in SH-SY5Y cells, suggested that pyroptosis may play an important role in the pathophysiological processes of drug-treated neuroblastoma [11]. As a dynamic nuclear protein, stimulus (e.g. chemoradiotherapy, ROS, autophagy, ferroptosis) promotes HMGB1 translocation from nucleus to cytosol, which participates in the regulation of cancer progression and chemosensitivity [17]. Here, our experimental data indicates that HMGB1 translocation is pyroptosis-dependent in SH-SY5Y cells. Knockdown of GSDME or pharmacological inhibition of caspase-3 activity suppressed DPP/VP16-induced pyroptosis limited HMGB1 translocation and release. Furthermore, knockdown of HMGB1 expression inhibited the DDP/VP16-induced generation of GSDME-N terminal fragments, and release of LDH, as well as the formation of large bubbles from the cellular membrane associated with pyroptosis. These results suggest that HMGB1 plays an important role in regulating pyroptosis of neuroblastoma cells.

GSDME, a gene associated with autosomal dominant nonsyndromic deafness, was newly identified as a promoter of pyroptosis owing to its cleavage by caspase-3 [8]. GSDME can also be used as a switch molecule in the transformation of apoptosis and pyroptosis. When it is highly expressed, cytotoxic drugs can induce

Endogenous HMGB1 regulates pyroptosis in neuroblastoma cells

tumor cell death through caspase-3-dependent pyroptosis. When the expression is low, the cell death mode is changed to apoptosis [11]. In cancer cell lines with high GSDME expression, such as SH-SY5Y cells and MeWo cells, the chemotherapy drugs, as an activator of caspase-3, can induce activated caspase-3 which cleaves GSDME instead of PARP [11]. Previous studies have shown that tumor cells that are prone to pyroptosis are more sensitive to chemotherapy drugs, suggesting that the occurrence of pyroptosis may be an indicator of chemosensitivity [32]. Here, we found that depletion of HMGB1 expression inhibited DDP/VP16-induced pyroptosis but increased the chemosensitivity and cleavage of PARP of DDP/VP16-treated cells, suggesting that knocking out HMGB1 switched DDP/VP16-induced cell death from pyroptosis to apoptosis.

ROS function as signaling molecules involved in regulating both cell survival and death through various pathways. ROS are also able to trigger PCD (apoptosis, autophagy, necroptosis, and ferroptosis), which causes cancer development, metastasis, and multidrug resistance during or after chemotherapy [33, 34]. Recently, mounting evidence has implied that the caspase-3/GSDME pathway is frequently associated with intracellular ROS production in cancerous cells. In melanoma cells, iron-activated ROS engender pyroptosis through the Tom20-Bax-caspase-GSDME pathway [29]. In triple-negative breast cancer cells, tetraarsenic hexoxide induces the pyroptotic cell death through activation of the mitochondrial ROS-mediated caspase-3/GSDME pathway, thereby suppressing tumor growth and metastasis [34]. The ERK1/2 pathway is involved in many cellular processes, including cell proliferation, differentiation, survival and death, and is an important target in the diagnosis and treatment of cancers [35, 36]. ERK1/2 signaling reportedly plays a pivotal role in caspase-3 activation, which contributes to GSDME-dependent pyroptosis. In a hepatocellular carcinoma cell line, miltirone inhibited the cell viability effectively elicited intracellular accumulation of ROS, and suppressed phosphorylation of MEK and ERK1/2 for GSDME-dependent pyroptosis induction [37]. Here, we found that DDP/VP16 potentially confers its pyroptotic activities via the ROS/ERK1/2/caspase-3/GSDME pathway in SH-SY5Y cells. We provide evidence that knockdown of HMGB1 inhibited

DDP/VP16-induced GSDME-NT, cleaved caspase-3 and p-REK1/2 expression in vitro and in vivo, all of which were reversed by pretreatment with the ROS agonist H₂O₂ and the ERK agonist EGF respectively. These pre-clinical results suggest that HMGB1-mediated pyroptosis represents a potential target for therapeutic interventions in neuroblastoma.

In summary, we show that HMGB1 was overexpressed in neuroblastoma cell lines and samples of patients with neuroblastoma and acted as a positive regulator of pyroptosis, which may enhance resistance to anti-cancer therapies. Knockdown of HMGB1 expression inhibited DDP/VP16-induced pyroptosis and switched cell death from pyroptosis to apoptosis, thereby increasing the chemosensitivity. HMGB1-mediated pyroptosis in DDP/VP16-treated cells regulated ROS generation and ERK1/2 phosphorylation in vitro and in vivo. The discovery of HMGB1 as a critical regulator of pyroptosis has provided new insights for therapeutic interventions in neuroblastoma.

Acknowledgements

This work was supported by the National Natural Science Foundation of China (No. 81770178 and No. 82002118), and The Natural Science Foundation of Hunan Province of China (No. 2020JJ4918 and No. 2021JJ40318).

Disclosure of conflict of interest

None.

Address correspondence to: Liang-Chun Yang, Department of Pediatrics, Xiangya Hospital, Central South University, Changsha 410008, Hunan, The People's Republic of China. Tel: +86-0731897537-58; Fax: +86-073189753758; E-mail: yangliangchung@163.com

References

- [1] Maris JM. Recent advances in neuroblastoma. *N Engl J Med* 2010; 362: 2202-2211.
- [2] Whittle SB, Smith V, Doherty E, Zhao S, McCarty S and Zage PE. Overview and recent advances in the treatment of neuroblastoma. *Expert Rev Anticancer Ther* 2017; 17: 369-386.
- [3] Zhang D, Kaweme NM, Duan P, Dong Y and Yuan X. Upfront treatment of pediatric high-risk neuroblastoma with chemotherapy, surgery,

Endogenous HMGB1 regulates pyroptosis in neuroblastoma cells

- and radiotherapy combination: the CCCG-NB-2014 protocol. *Front Oncol* 2021; 11: 745794.
- [4] Jorgensen I and Miao EA. Pyroptotic cell death defends against intracellular pathogens. *Immunol Rev* 2015; 265: 130-142.
- [5] Volchuk A, Ye A, Chi L, Steinberg BE and Goldenberg NM. Indirect regulation of HMGB1 release by gasdermin D. *Nat Commun* 2020; 11: 4561.
- [6] Tsuchiya K. Switching from apoptosis to pyroptosis: gasdermin-elicited inflammation and antitumor immunity. *Int J Mol Sci* 2021; 22: 426.
- [7] Shi J, Zhao Y, Wang K, Shi X, Wang Y, Huang H, Zhuang Y, Cai T, Wang F and Shao F. Cleavage of GSDMD by inflammatory caspases determines pyroptotic cell death. *Nature* 2015; 526: 660-665.
- [8] De Schutter E, Croes L, Ibrahim J, Pauwels P, Op de Beeck K, Vandenabeele P and Van Camp G. GSDME and its role in cancer: from behind the scenes to the front of the stage. *Int J Cancer* 2021; 148: 2872-2883.
- [9] Akino K, Toyota M, Suzuki H, Imai T, Maruyama R, Kusano M, Nishikawa N, Watanabe Y, Sasaki Y, Abe T, Yamamoto E, Tarasawa I, Sonoda T, Mori M, Imai K, Shinomura Y and Tokino T. Identification of DFNA5 as a target of epigenetic inactivation in gastric cancer. *Cancer Sci* 2007; 98: 88-95.
- [10] Masuda Y, Futamura M, Kamino H, Nakamura Y, Kitamura N, Ohnishi S, Miyamoto Y, Ichikawa H, Ohta T, Ohki M, Kiyono T, Egami H, Baba H and Arakawa H. The potential role of DFNA5, a hearing impairment gene, in p53-mediated cellular response to DNA damage. *J Hum Genet* 2006; 51: 652-664.
- [11] Wang Y, Gao W, Shi X, Ding J, Liu W, He H, Wang K and Shao F. Chemotherapy drugs induce pyroptosis through caspase-3 cleavage of a gasdermin. *Nature* 2017; 547: 99-103.
- [12] Lage H, Helmbach H, Grottko C, Dietel M and Schadendorf D. DFNA5 (ICERE-1) contributes to acquired etoposide resistance in melanoma cells. *FEBS Lett* 2001; 494: 54-59.
- [13] Zhang CC, Li CG, Wang YF, Xu LH, He XH, Zeng QZ, Zeng CY, Mai FY, Hu B and Ouyang DY. Chemotherapeutic paclitaxel and cisplatin differentially induce pyroptosis in A549 lung cancer cells via caspase-3/GSDME activation. *Apoptosis* 2019; 24: 312-325.
- [14] Rogers C, Erkes DA, Nardone A, Aplin AE, Fernandes-Alnemri T and Alnemri ES. Gasdermin pores permeabilize mitochondria to augment caspase-3 activation during apoptosis and inflammasome activation. *Nat Commun* 2019; 10: 1689.
- [15] Yu J, Li S, Qi J, Chen Z, Wu Y, Guo J, Wang K, Sun X and Zheng J. Cleavage of GSDME by caspase-3 determines lobaplatin-induced pyroptosis in colon cancer cells. *Cell Death Dis* 2019; 10: 193.
- [16] Lotze MT and Tracey KJ. High-mobility group box 1 protein (HMGB1): nuclear weapon in the immune arsenal. *Nat Rev Immunol* 2005; 5: 331-342.
- [17] Tang D, Kang R, Zeh HJ 3rd and Lotze MT. High-mobility group box 1 and cancer. *Biochim Biophys Acta* 2010; 1799: 131-140.
- [18] Tang D, Kang R, Livesey KM, Cheh CW, Farkas A, Loughran P, Hoppe G, Bianchi ME, Tracey KJ, Zeh HJ 3rd and Lotze MT. Endogenous HMGB1 regulates autophagy. *J Cell Biol* 2010; 190: 881-892.
- [19] Yang L, Chai W, Wang Y, Cao L, Xie M, Yang M, Kang R and Yu Y. Reactive oxygen species regulate the differentiation of acute promyelocytic leukemia cells through HMGB1-mediated autophagy. *Am J Cancer Res* 2015; 5: 714-725.
- [20] Kang R, Chen R, Zhang Q, Hou W, Wu S, Cao L, Huang J, Yu Y, Fan XG, Yan Z, Sun X, Wang H, Wang Q, Tsung A, Billiar TR, Zeh HJ 3rd, Lotze MT and Tang D. HMGB1 in health and disease. *Mol Aspects Med* 2014; 40: 1-116.
- [21] Ye F, Chai W, Xie M, Yang M, Yu Y, Cao L and Yang L. HMGB1 regulates erastin-induced ferroptosis via RAS-JNK/p38 signaling in HL-60/NRAS(Q61L) cells. *Am J Cancer Res* 2019; 9: 730-739.
- [22] Wang L, Zhang H, Sun M, Yin Z and Qian J. High mobility group box 1-mediated autophagy promotes neuroblastoma cell chemoresistance. *Oncol Rep* 2015; 34: 2969-2976.
- [23] Liu Y and Song L. HMGB1-induced autophagy in Schwann cells promotes neuroblastoma proliferation. *Int J Clin Exp Pathol* 2015; 8: 504-510.
- [24] Tang L, Chai W, Ye F, Yu Y, Cao L, Yang M, Xie M and Yang L. HMGB1 promotes differentiation syndrome by inducing hyperinflammation via MEK/ERK signaling in acute promyelocytic leukemia cells. *Oncotarget* 2017; 8: 27314-27327.
- [25] Yang L, Yu Y, Kang R, Yang M, Xie M, Wang Z, Tang D, Zhao M, Liu L, Zhang H and Cao L. Up-regulated autophagy by endogenous high mobility group box-1 promotes chemoresistance in leukemia cells. *Leuk Lymphoma* 2012; 53: 315-322.
- [26] Yang L, Ye F, Zeng L, Li Y and Chai W. Knockdown of HMGB1 suppresses hypoxia-induced mitochondrial biogenesis in pancreatic cancer cells. *Onco Targets Ther* 2020; 13: 1187-1198.
- [27] Chai W, Ye F, Zeng L, Li Y and Yang L. HMGB1-mediated autophagy regulates sodium/iodide

Endogenous HMGB1 regulates pyroptosis in neuroblastoma cells

- symporter protein degradation in thyroid cancer cells. *J Exp Clin Cancer Res* 2019; 38: 325.
- [28] Goldar S, Khaniani MS, Derakhshan SM and Baradaran B. Molecular mechanisms of apoptosis and roles in cancer development and treatment. *Asian Pac J Cancer Prev* 2015; 16: 2129-2144.
- [29] Zhou B, Zhang JY, Liu XS, Chen HZ, Ai YL, Cheng K, Sun RY, Zhou D, Han J and Wu Q. Tom20 senses iron-activated ROS signaling to promote melanoma cell pyroptosis. *Cell Res* 2018; 28: 1171-1185.
- [30] Jo SK, Cho WY, Sung SA, Kim HK and Won NH. MEK inhibitor, U0126, attenuates cisplatin-induced renal injury by decreasing inflammation and apoptosis. *Kidney Int* 2005; 67: 458-466.
- [31] Ma L, Bian M, Gao H, Zhou Z and Yi W. A novel 3-acyl isoquinolin-1(2H)-one induces G2 phase arrest, apoptosis and GSDME-dependent pyroptosis in breast cancer. *PLoS One* 2022; 17: e0268060.
- [32] Wu M, Wang Y, Yang D, Gong Y, Rao F, Liu R, Danna Y, Li J, Fan J, Chen J, Zhang W and Zhan Q. A PLK1 kinase inhibitor enhances the chemosensitivity of cisplatin by inducing pyroptosis in oesophageal squamous cell carcinoma. *EBioMedicine* 2019; 41: 244-255.
- [33] Szakacs G, Paterson JK, Ludwig JA, Booth-Genthe C and Gottesman MM. Targeting multi-drug resistance in cancer. *Nat Rev Drug Discov* 2006; 5: 219-234.
- [34] An H, Heo JS, Kim P, Lian Z, Lee S, Park J, Hong E, Pang K, Park Y, Ooshima A, Lee J, Son M, Park H, Wu Z, Park KS, Kim SJ, Bae I and Yang KM. Tetraarsenic hexoxide enhances generation of mitochondrial ROS to promote pyroptosis by inducing the activation of caspase-3/GSDME in triple-negative breast cancer cells. *Cell Death Dis* 2021; 12: 159.
- [35] Dhillon AS, Hagan S, Rath O and Kolch W. MAP kinase signalling pathways in cancer. *Oncogene* 2007; 26: 3279-3290.
- [36] Sun Y, Liu WZ, Liu T, Feng X, Yang N and Zhou HF. Signaling pathway of MAPK/ERK in cell proliferation, differentiation, migration, senescence and apoptosis. *J Recept Signal Transduct Res* 2015; 35: 600-604.
- [37] Zhang X, Zhang P, An L, Sun N, Peng L, Tang W, Ma D and Chen J. Miltirone induces cell death in hepatocellular carcinoma cell through GSDME-dependent pyroptosis. *Acta Pharm Sin B* 2020; 10: 1397-1413.

Endogenous HMGB1 regulates pyroptosis in neuroblastoma cells

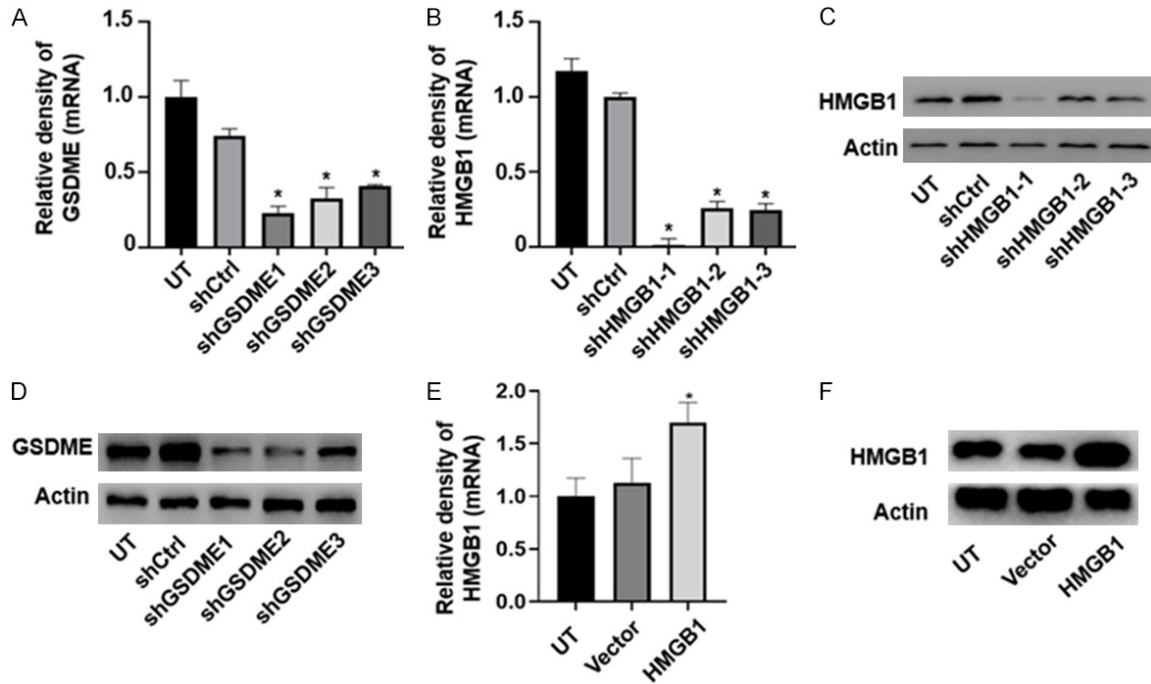


Figure S1. Verification of GSDME and HMGB1 gene transfection in SH-SY5Y cells. A and B. SH-SY5Y cells were incubated with HIV-eGFP-GSDME or HIV-eGFP-HMGB1 for 48 h at a MOI of 20. After gene stable transfection, GSDME or HMGB1 level was detected by qRT-PCR. Actin was a loading control. UT: untransfected group. (n = 3, **P* < 0.05 vs. shCtrl group). C and D. SH-SY5Y cells were incubated with HIV-eGFP-GSDME or HIV-eGFP-HMGB1 for 48 h at a MOI of 20. After gene stable transfection, GSDME or HMGB1 level was detected by western blot. Actin was a loading control. UT: untransfected group. E and F. SH-SY5Y cells were transfected with HMGB1 vector or empty vector. After gene stable transfection, HMGB1 level was detected by western blot and qRT-PCR. Actin was a loading control. UT: untransfected group. (n = 3, **P* < 0.05 vs. vector group).

Endogenous HMGB1 regulates pyroptosis in neuroblastoma cells

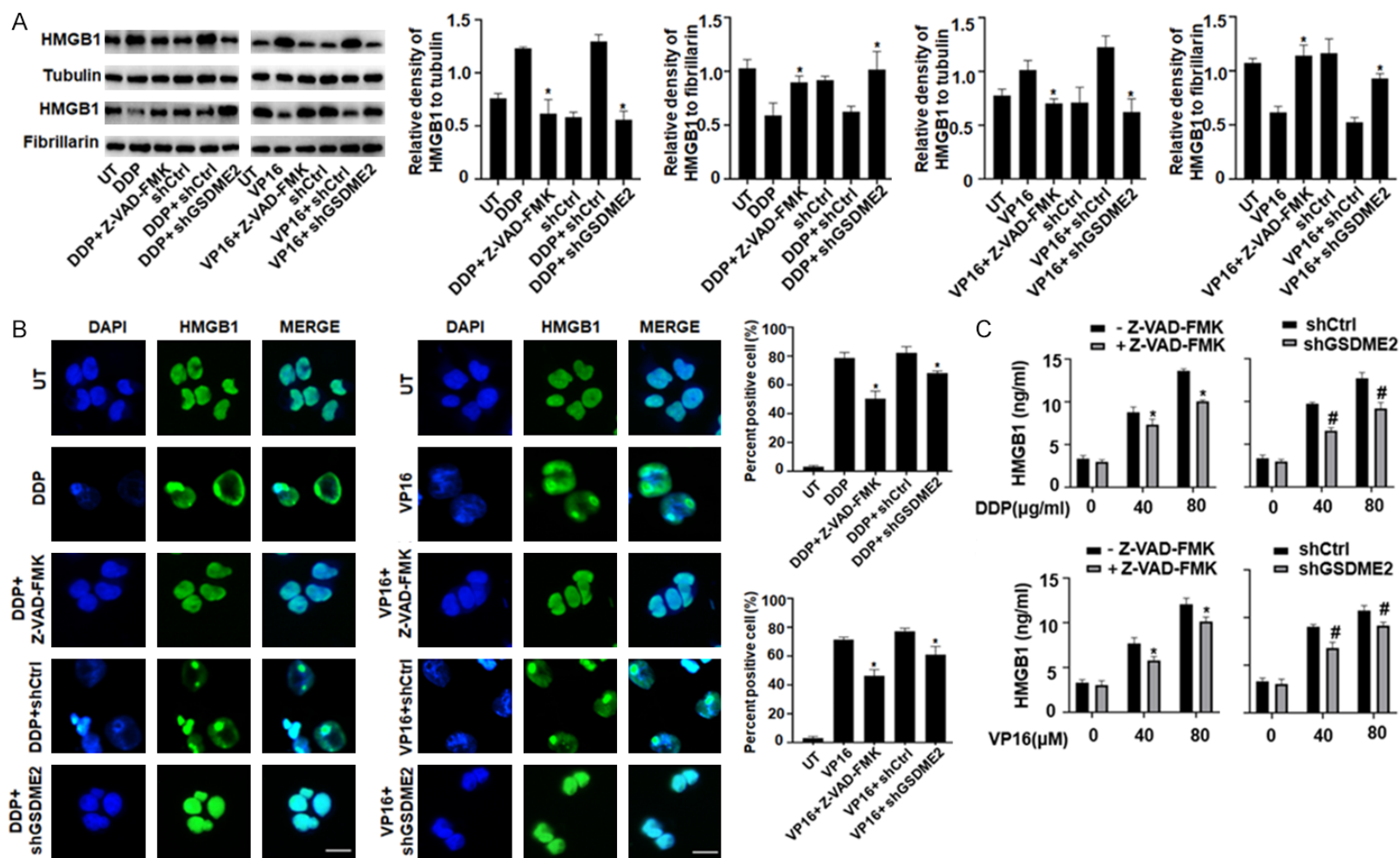


Figure S2. DDP/VP16-induced pyroptosis is required for HMGB1 translocation and release. A and B. SH-SY5Y cells were transfected with GSDME2 shRNA and control shRNA, or pretreated with or without Z-VAD-FMK (10 μM) for 24 h, and then treated with DDP (40 μg/ml) and VP16 (40 μM) for 24 h, respectively. The nuclear/cytoplasmic HMGB1 protein expression was assayed by western blot and immunofluorescence (Green, HMGB1; blue, nucleus). Scale bars, 100 μm; (n = 3, *P < 0.05 vs. DDP or VP16 treatment group; #P < 0.05 vs. shCtrl group). C. SH-SY5Y cells were transfected with GSDME2 shRNA and control shRNA, or pretreated with or without Z-VAD-FMK (10 μM) for 24 h, and then treated with DDP and VP16 at the indicated doses for 24 h, respectively. The release of HMGB1 was analyzed by ELISA (n = 3, *P < 0.05 vs. Z-VAD-FMK treatment group; #P < 0.05 vs. shCtrl group).

Endogenous HMGB1 regulates pyroptosis in neuroblastoma cells

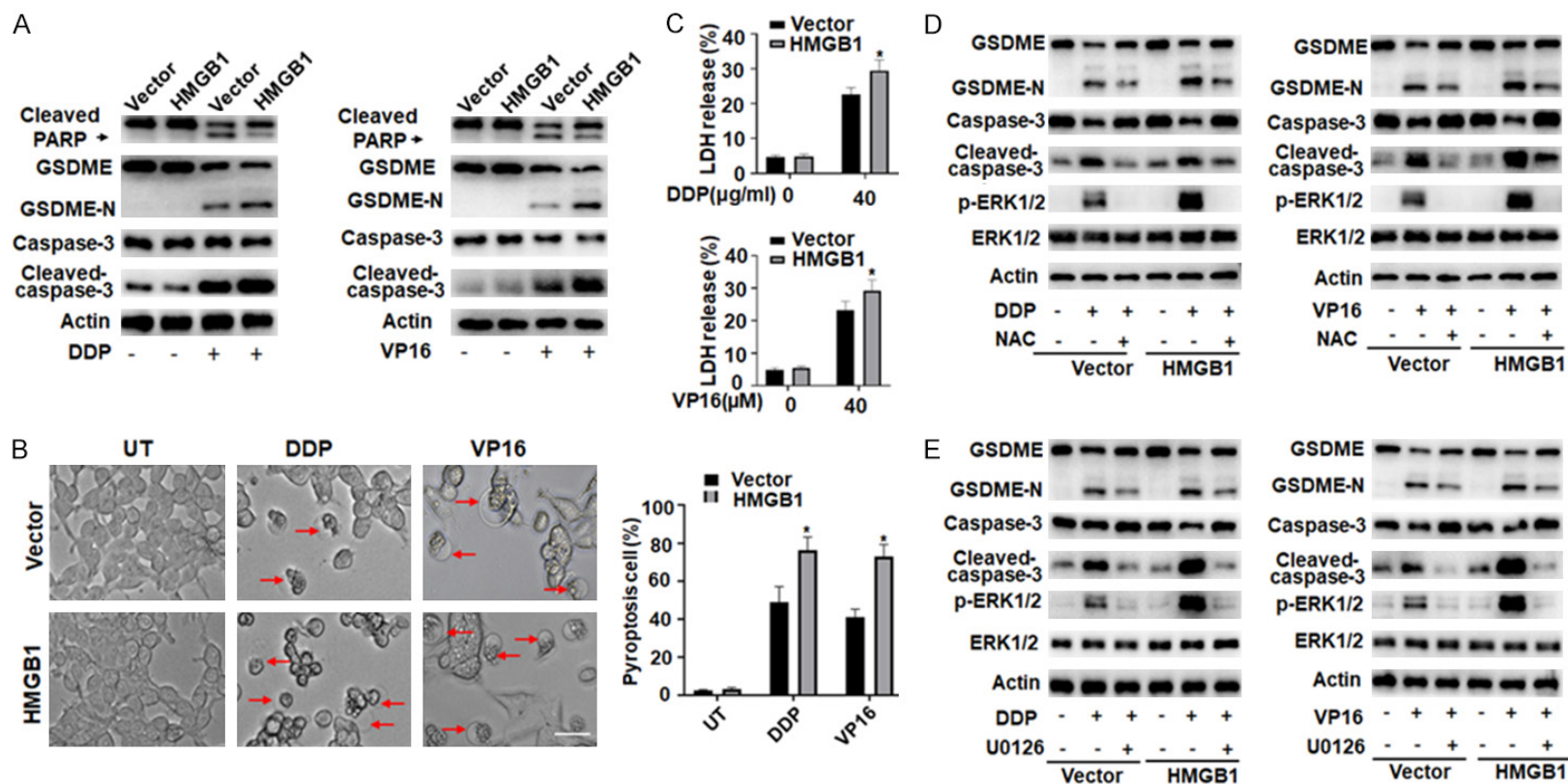


Figure S3. Up-regulated HMGB1 promote DDP/VP16-induced pyroptosis in a ROS-ERK1/2 pathway. **A.** SH-SY5Y cells treated with DDP (40 $\mu\text{g/ml}$) and VP16 (40 μM) for 24 h in HMGB1 vector or empty vector groups, respectively. GSDME-NT, cleaved caspase-3 and cleaved PARP levels were assayed by western blot. **B.** Representative light microscopy images of HMGB1 vector or empty vector groups with differently treatments were detected. The red arrow indicates bubbles emerging from the plasma membrane. ($n = 3$, $*P < 0.05$ vs. vector group). **C.** HMGB1 vector or empty vector groups of LDH-release was analyzed using LDH assay kit and expressed as mean \pm SD ($n = 3$, $*P < 0.05$ vs. vector group). **D** and **E.** HMGB1 vector group and empty vector groups were pretreated with or without NAC (10 μM) and U0126 (10 μM) for 12 h, and then treated with DDP (40 $\mu\text{g/ml}$) and VP16 (40 μM) for 24 h, respectively. GSDME-NT, cleaved caspase-3 and p-ERK1/2 levels were assayed by western blot.

Endogenous HMGB1 regulates pyroptosis in neuroblastoma cells

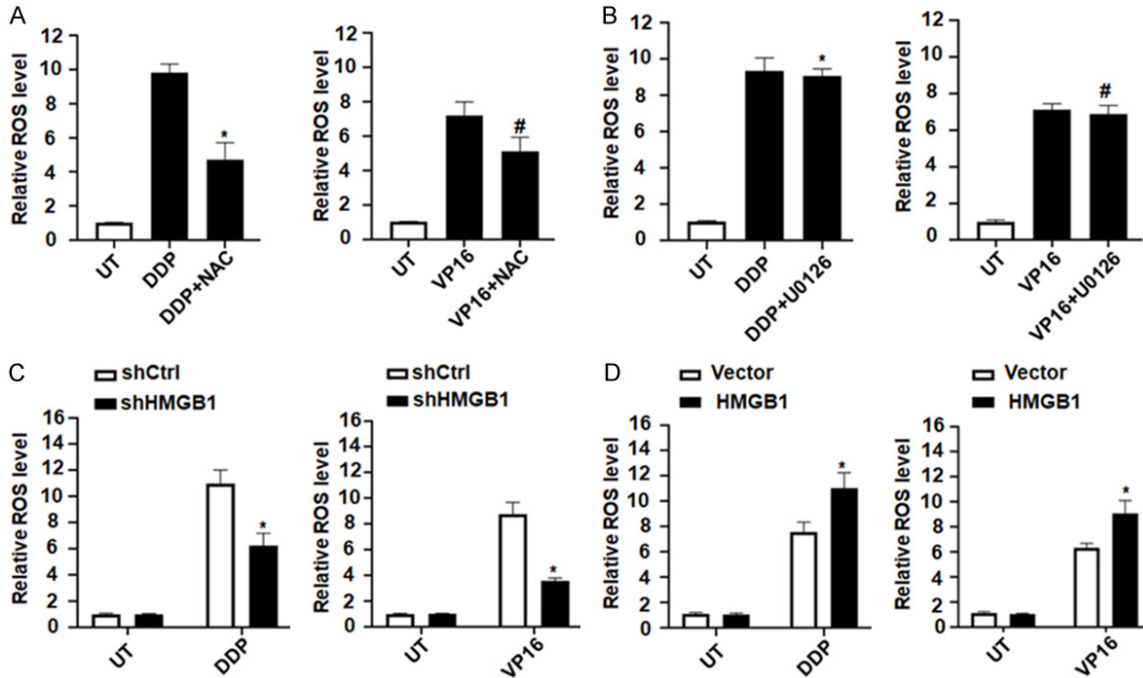


Figure S4. ROS is involved in HMGB1-mediated pyroptosis in response to chemotherapy drugs through ROS/ERK1/2/caspase-3/GSDME pathway. A. SH-SY5Y cells were pretreated with or without NAC (20 μ M) for 12 h, and then treated with DDP (40 μ g/ml) and VP16 (40 μ M) for 24 h, respectively. ROS production was measured by a ROS Assay. (n = 3, * P < 0.05 vs. DDP group; * P < 0.05 vs. VP16 group). B. SH-SY5Y cells were pretreated with or without U0126 (10 μ M) for 12 h, and then treated with DDP (40 μ g/ml) and VP16 (40 μ M) for 24 h, respectively. ROS production was measured by a ROS Assay. (n = 3, * P > 0.05 vs. DDP group; # P > 0.05 vs. VP16 group). C. SH-SY5Y cells were transfected with HMGB1 shRNA and control shRNA, and then treated with DDP (40 μ g/ml) and VP16 (40 μ M) for 24 h, respectively. ROS production was measured by a ROS Assay. (n = 3, * P < 0.05 vs. shCtrl group). D. SH-SY5Y cells were transfected with HMGB1 vector shRNA and empty vector, and then treated with DDP (40 μ g/ml) and VP16 (40 μ M) for 24 h, respectively. ROS production was measured by a ROS Assay. (n = 3, * P < 0.05 vs. vector group).